VOL. 12, NO. 22, NOVEMBER 2017 ISSN 1819-6608
ARPN Journal of Engineering and Applied Sciences

www.arpnjournals.com

IMPLEMENTATION OF OCTAGONAL AND HEXAGONAL STRIP MONOPOLE ANTENNAS FOR UWB APPLICATIONS

K. S. Chakradhar[1] and B. Rama Rao[2]
[1]Sree Vidyanikethan Engineering College, Tirupathi, Andhra Pradesh, India
[2]Aditya Institute of Technology and Management Tekkali, Andhra Pradesh, India
E-Mail: chakradharec@gmail.com

ABSTRACT

Ultra-wideband (UWB) communication systems have the promise of very high bandwidth, reduced fading from multipath and low power requirements. Band width can be extended to higher frequencies by adding a Octagonal or Hexagonal strip horizontally from the printed radiator and asymmetrically attaching a conducting strip to the radiator. This paper reports about the design of the antennas to enhance the bandwidth by increasing the size of the strip monopole by different geometries. The geometry of the wide octagonal strip monopole is a Octagon of side 'a=9mm' where as for the wide hexagon monopole is a hexagon of side 'a=10mm'.The strip length is 23mm and small gap 'd=3mm' between ground planes and strip for both the antenna geometries to achieve matching. The two printed monopole antennas are designed are etched onto a FR-4 epoxy substrate with an overall size of 45mm × 60mm ×1.6 mm. The proposed antennas are simulated using Ansoft HFSS and the practical results are obtained by testing the patches on vector network analyzer. The hexagonal strip monopole is resonating at 5.5 GHz and UWB impedance bandwidth ($S11 < -10$ dB) ranges from 1.54 to 9.41GHz, while the octagonal strip monopole is resonating at 5.5GHz and UWB impedance bandwidth ($S11 < -10$ dB) ranges from 1.3 to 5.65 GHz. The VSWR values for hexagonal is 1.52:1 at 2.09GHz & for octagonal it is 1.53:1 at 1.78GHz.The bandwidth for hexagonal is 7.87GHz, while for octagonal is 4.35GHz.

Keywords: octagonal, hexagonal, UWB, HFSS.

1. INTRODUCTION

Since the declaration of ultra-wideband (UWB) frequencies (from 3.1 GHz to 10.6 GHz) by the federal communications commission (FCC) in 2002 [1], antenna design for this new communications standard has attracted increasing interest. Commercial UWB systems require small low-cost antennas with Omni directional radiation patterns, large bandwidth and non-dispersive behaviour [2]. These requirements make UWB antenna design more complicated than traditional narrow-band designs. An antenna is a key element for wireless communication as it transmits and/or receives electromagnetic waves [3]. Several antenna designs have been developed during a decade, for their application depends on the physical parameters of its output. Due to recent trends of the communication system requirements in portable devices, it is necessary to design a light, compact, portable and an efficient antenna [4]. Many researchers are still developing optimum designs to reduce the size and weight of multi band antennas while keeping good performances [5-7]. An integrated antenna is among the one that is being preferred due to several practical applications, because of its light weight, small size, easy to fabrication and cheap realization. A small integrated antenna called as microstrip antenna has significant applications in the area of wireless communication and is used for several microwave applications. The construction of microstrip antenna is easy as it requires a thin patch on one side of a dielectric substrate. The other side of substrate has a plane to the ground [8]. The patch is generally made of conducting material like Copper or Gold and may be in any arbitrary shapes like rectangular, circular, triangular and elliptical or some other shape [9]. For practical applications, the most common used microstrip patches are rectangular and circular patch antennas. In wireless communication, small integrated antennas are preferred than other radiating systems., due to their light weight, reduced size, low cost, conformability and ease of integration with communication devices [10].

Several studies on printed wide-slot antennas indicated that the impedance bandwidth of the antenna is controlled by the coupling between the tuning stub and the slot. Bandwidth enhancement is achieved by employing a feeding scheme that generates multiple resonances. By optimizing the distance between the tuning stub and ground surrounding it, the impedance changes from one resonant mode to the other is minimized, resulting in wideband operation. Forklike, circular, elliptical rectangular and inverted cone shapes of the tuning stubs have been reported [11], [12] In this paper [13], the self-similarity property of the fractal technology is used to construct the multi-frequency antenna structure to realize the UWB characteristic under the standard mask set by FCC.

2. PRINCIPLE OF OPERATION OF MICROSTRIP ANTENNA

The patch acts approximately as a resonant cavity with short-circuit (PEC) walls on top and bottom, open-circuit (PMC) walls on the edges. In a cavity, only certain modes are allowed to exist, at different resonance frequencies. If the antenna is excited at a resonance frequency, a strong field is set up inside the cavity, and a strong current on the (bottom) surface of the patch. This produces significant radiation (a good antenna).

VOL. 12, NO. 22, NOVEMBER 2017 ISSN 1819-6608
ARPN Journal of Engineering and Applied Sciences

Thin substrate approximation

On patch and ground plane, the tangential Electric field is Zero this can be expressed as

$$\underline{E}_t = \underline{0} \text{ and } \quad \underline{E} = \hat{\underline{z}} E_z$$

Inside the patch cavity, because of the thin substrate, the electric field vector is approximately independent of *z*. and hence

$$\underline{E}(x,y,z) \approx \hat{\underline{z}} E_z(x,y)$$

Magnetic field inside patch cavity is given by

$$\underline{H} = -\frac{1}{j\omega\mu}\nabla\times\underline{E}$$
$$= -\frac{1}{j\omega\mu}\nabla\times\left(\hat{\underline{z}}E_z(x,y)\right)$$
$$= -\frac{1}{j\omega\mu}\left(-\hat{\underline{z}}\times\nabla E_z(x,y)\right)$$
$$\underline{H}(x,y) = \frac{1}{j\omega\mu}\left(\hat{\underline{z}}\times\nabla E_z(x,y)\right)$$

On the edges of the patch

$$\underline{J}_s \cdot \hat{\underline{n}} = 0$$

Where $\underline{J}_s$ is the sum of the top and bottom surface currents of the patch. On the bottom surface of the patch conductor, at the edge on the patch, we have

$$\underline{J}_s^{bot} \cdot \hat{\underline{n}} \approx \underline{0}$$

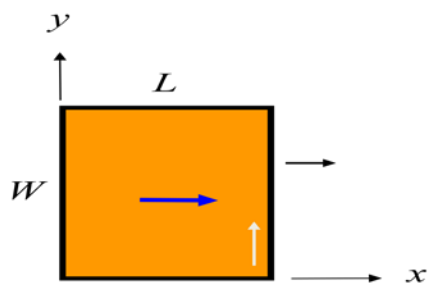

$$\left(\text{assuming } \left|\underline{J}_s^{bot}\right| >> \left|\underline{J}_s^{top}\right|\right)$$

Also,

$$\underline{J}_s^{bot} = \left(-\hat{\underline{z}}\times\underline{H}\right)$$
$$\underline{H}_t^{bot} \approx \underline{0}$$

Magnetic-wall approximation

Since the magnetic field is approximately independent of *z*, it has an approximate PMC condition on the entire vertical edge

$$\underline{H}_t = \underline{0} \quad \text{(PMC)} \quad \hat{\underline{n}}\times\underline{H}(x,y) = \underline{0}$$

or

$$\hat{\underline{n}}\times\underline{H}(x,y) = \underline{0}$$
$$\underline{H}(x,y) = \frac{1}{j\omega\mu}\left(\hat{\underline{z}}\times\nabla E_z(x,y)\right)$$

And Hence $\hat{\underline{n}}\times\left(\hat{\underline{z}}\times\nabla E_z(x,y)\right) = \underline{0}$

$$\hat{\underline{n}}\times\left(\hat{\underline{z}}\times\nabla E_z(x,y)\right) = \hat{\underline{z}}\left(\hat{\underline{n}}\cdot\nabla E_z(x,y)\right) - \nabla E_z(x,y)\left(\hat{\underline{n}}\cdot\hat{\underline{z}}\right)$$
$$\hat{\underline{z}}\left(\hat{\underline{n}}\cdot\nabla E_z(x,y)\right) = \underline{0}$$
$$\frac{\partial E_z}{\partial n} = 0$$

Resonance frequencies

The resonance frequencies of the patch can obtained by considering the wave equation

$$\nabla^2 E_z + k^2 E_z = 0$$

From separation of variables, we can get

$$E_z = \cos\left(\frac{m\pi x}{L}\right)\cos\left(\frac{n\pi y}{W}\right)$$

this equation is for TM_{mn} mode
then have

$$\left[-\left(\frac{m\pi}{L}\right)^2 - \left(\frac{n\pi}{W}\right)^2 + k_1^2\right]E_z = 0$$
$$\left[-\left(\frac{m\pi}{L}\right)^2 - \left(\frac{n\pi}{W}\right)^2 + k_1^2\right] = 0$$

thus have

$$k_1^2 = \left(\frac{m\pi}{L}\right)^2 + \left(\frac{n\pi}{W}\right)^2$$

Re call that $k_1 = k_0\sqrt{\varepsilon_r} = \omega\sqrt{\mu_0\varepsilon_0}\sqrt{\varepsilon_r}$
Hence

$$f = \frac{c}{2\pi\sqrt{\varepsilon_r}}\sqrt{\left(\frac{m\pi}{L}\right)^2 + \left(\frac{n\pi}{W}\right)^2}$$

Where $c = 1/\sqrt{\mu_0 \varepsilon_0}$

Hence $f = f_{mn}$

The resonance frequency of (*m*,*n*) mode)

$$f_{mn} = \frac{c}{2\pi\sqrt{\varepsilon_r}} \sqrt{\left(\frac{m\pi}{L}\right)^2 + \left(\frac{n\pi}{W}\right)^2}$$

Dominant (1, 0) mode

This structure operates as a "fat planar dipole."

This mode is usually used because the radiation pattern has a broadside beam.

$$f_{10} = \frac{c}{2\sqrt{\varepsilon_r}} \left(\frac{1}{L}\right)$$

$$E_z = \cos\left(\frac{\pi x}{L}\right)$$

$$\underline{H}(x, y) = -\underline{\hat{y}} \left(\frac{1}{j\omega\mu}\right)\left(\frac{\pi}{L}\right)\sin\left(\frac{\pi x}{L}\right)$$

The resonant length *L* is about 0.5 guided wavelengths in the *x* direction

$$\underline{J}_s = \underline{\hat{x}} \left(\frac{-1}{j\omega\mu_0}\right)\left(\frac{\pi}{L}\right)\sin\left(\frac{\pi x}{L}\right)$$

Resonance frequency of dominant mode

The resonance frequency is mainly controlled by the patch length L and the substrate permittivity. Approximately, (assuming PMC walls)

$$k_1^2 = \left(\frac{m\pi}{L}\right)^2 + \left(\frac{n\pi}{W}\right)^2$$

(1,0) mode: $k_1 L = \pi$

$$L = \lambda_d / 2 = \frac{\lambda_0 / 2}{\sqrt{\varepsilon_r}}$$

This is equivalent to saying that the length L is one-half of a wavelength in the dielectric. A higher substrate permittivity allows for a smaller antenna miniaturization with a lower bandwidth. The resonance frequency calculation can be improved by adding a "fringing length extension" ΔL to each edge of the patch to get an "effective length" L_e.

$$L_e = L + 2\Delta L$$

$$f_{10} = \frac{c}{2\sqrt{\varepsilon_r}} \left(\frac{1}{L_e}\right)$$

Hammerstad formula:

$$\Delta L / h = 0.412 \left[\frac{\left(\varepsilon_r^{eff} + 0.3\right)\left(\frac{W}{h} + 0.264\right)}{\left(\varepsilon_r^{eff} - 0.258\right)\left(\frac{W}{h} + 0.8\right)}\right]$$

$$\varepsilon_r^{eff} = \frac{\varepsilon_r + 1}{2} + \left(\frac{\varepsilon_r - 1}{2}\right)\left[1 + 12\left(\frac{h}{W}\right)\right]^{-1/2}$$

Even though the Hammerstad formula involves an effective permittivity, we still use the actual substrate permittivity in the resonance frequency formula.

$$f_{10} = \frac{c}{2\sqrt{\varepsilon_r}} \left(\frac{1}{L + 2\Delta L}\right)$$

Note that

$$\Delta L \approx 0.5\ h$$

This is a good "rule of thumb" to give a quick estimate

3. ANTENNA DESIGN SPICIFICATONS

The geometry of the proposed antenna with its parameter is depicted in Figures 1 and 2. The fabrication of the proposed antenna is done using a conventional FR4 substrate, often used to make printed circuit boards with thickness (*h*) of 1.6mmand relative permittivity of 4.4, which makes it easy and inexpensive to manufacture. The three essential parameters for the design of a microstrip Antennas are:

Resonant frequency (*fr*): The resonant frequency of the antenna must be selected appropriately. The Ultra wideband (UWB) communication systems have the frequency range from3.1GHz to 10.6 GHz; hence the antenna designed must be able to operate in this frequency range. The resonant frequency selected for design is 5.5 GHz,

Dielectric constant of the substrate (€r): The dielectric material selected for our design is FR4 epoxy which has a dielectric constant of 4.4. A substrate with a high dielectric constant has been selected since it reduces the dimensions of the antenna.

- Height of dielectric substrate (h): For the microstrip Patch antenna to be used in wireless applications, it is

VOL. 12, NO. 22, NOVEMBER 2017 ISSN 1819-6608
ARPN Journal of Engineering and Applied Sciences

essential that the antenna is not bulky. Hence, the height of the dielectric substrate is selected as 1.6 mm. Hence, the essential parameters for the design are:

- *fo* = 5.5 GHz
- €*r* = 4.4
- *h* = 1.6 mm

Step 1: Calculation of the effective dielectric constant (€r):

Equation (1) gives the effective dielectric constant as:

$$\in_{eff} = \frac{\in_r + 1}{2}(1 + 0.3 * h) \quad (1)$$

Step2: Calculation of the length of strip (Ls*)*:

The length of the Microstrip antenna given by the equation (2)

$$Ls = \frac{0.42 * c}{f_r * \sqrt{\in_{eff}}} \quad (2)$$

Step 3: Calculation of the width of ground plane (Wg):

The width of the ground plane can be calculated by the equation (3)

$$W_g = \frac{1.38 * c}{f_r * \sqrt{\in_{eff}}} \quad (3)$$

Step 4: Calculation of the length of ground plane (Lg):

Here the length of the ground plane is obtained by equation (4)

$$Lg = \frac{0.36 * c}{f_r * \sqrt{\in_{eff}}} \quad (4)$$

Step 5: Calculation of the resonant frequency (fr*)*:

Resonant frequency (fr) is given by the equation (5),

$$f_r = 3 + \frac{2}{\sqrt{\in_{ref}}}\left[\frac{21}{Ls} + \frac{65}{Wg} + \frac{18}{Lg} - 3\right] \quad (5)$$

By using the design equations the dimensions of strip monopole antenna are having the values of a=10 mm for hexagonal and a=9 mm for octagonal antennas and Wg=45mm, Lg=20mm, D=3mm, H=9mm, A=1.6mm, ε_r= 4.44

a) Design of octagonal microstrip antenna

The geometry of proposed finite ground coplanar waveguide (CPW) fed dual-band Octagonal monopole antenna is shown in Figure-3. The antenna structure is chosen to be a rectangular patch element with dimensions of width W and length L, and with a vertical spacing of 'h' away from the ground plane. A conventional CPW fed line designed with a gap of distance a 'd' between the signal strip and the coplanar ground plane is used for exciting the radiating patch element. Two finite ground planes with the same size of width Wg and length Lg are situated symmetrically on each side of the CPW feeding line. The Table-1 shows the dimensions of the proposed octagonal antenna.

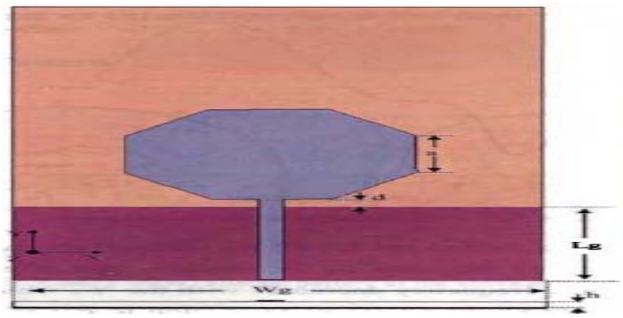

Figure-1. Wide octagonal strip monopole antenna.

Table-1. Dimensions of the proposed octagonal strip monopole antenna.

Configuration	Parameters	Dimensions
Substrate	W L h ε_r	60mm 45mm 1.6mm 4.38mm
Ground plane	W_g L_g	45mm 20mm
Antenna	D a	3mm 9mm

b) Dsign of hexagonal microstrip antenna

The geometry of the proposed finite ground coplanar wave guide (CPW) fed dual-band Hexagonal monopole antenna shown in Figure-4. The proposed antenna was fabricated on FR4 substrate with dielectric constant 4.4 and thickness 1.6 mm.

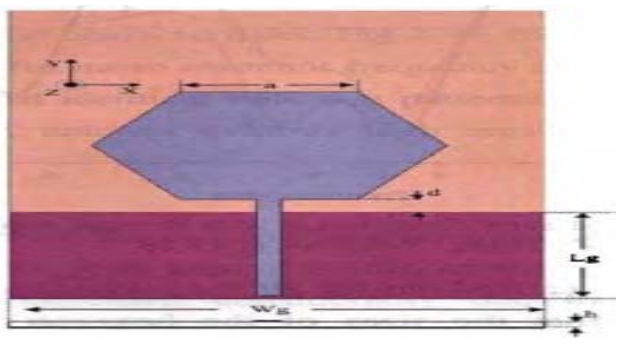

Figure-2. Wide hexagonal strip monopole antenna.

VOL. 12, NO. 22, NOVEMBER 2017 ISSN 1819-6608
ARPN Journal of Engineering and Applied Sciences

www.arpnjournals.com

The Table-2 shows the dimensions of the proposed Hexagonal antenna.

Table-2. Dimensions of the proposed hexagonal strip antenna.

Configuration	Parameters	Dimensions
Substrate	W L h ε_r	60mm 45mm 1.6mm 4.38mm
Ground plane	W_g L_g	45mm 20mm
Antenna	D a	1mm 10mm

4. RESULTS

Prototypes of the octagonal and hexagonal shape antennas are simulated constructed and tested. The proposed antenna is simulated using HFSS, Figures 1, 2 shows the simulated antennas.

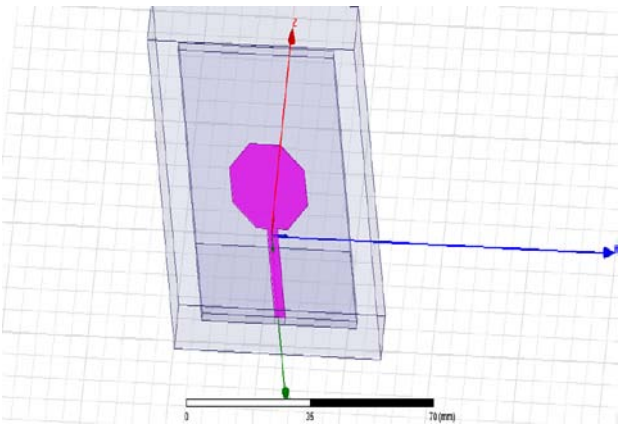

Figure-3. HFSS modal of octagonal antenna.

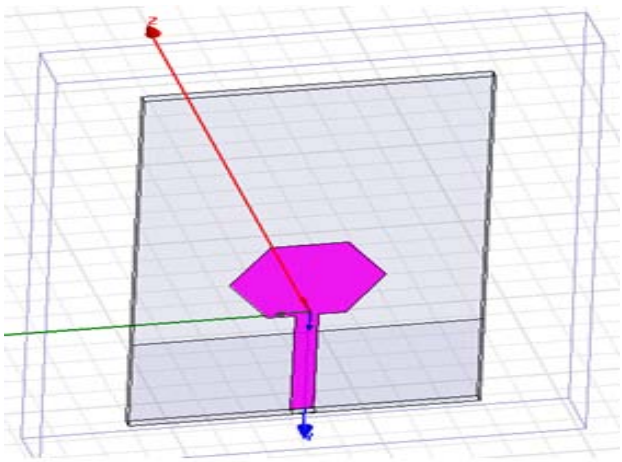

Figure-4. HFSS modal of hexagonal antenna.

A. Octagonal strip monopole antenna

The performance of the octagonal shape antenna has been investigated by using HFSS. The figures 5, 6 shows the simulated return loss, VSWR and figures 7, 8 shows the tested return loss, VSWR and the figure-9 shows the radiation pattern of the strip monopole antenna from the frequency 1.9 GHz to 9.4 GHz.

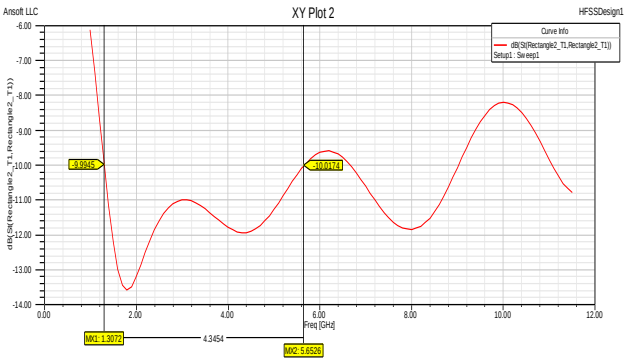

Figure-5. Return loss curve for wide octagonal strip monopole antenna using HFSS.

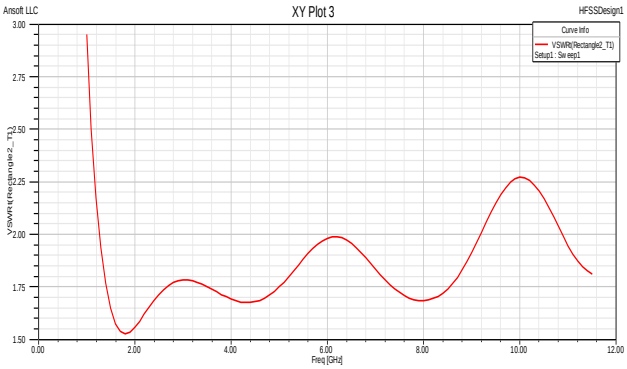

Figure-6. VSWR curve for wide octagonal strip monopole antenna using HFSS.

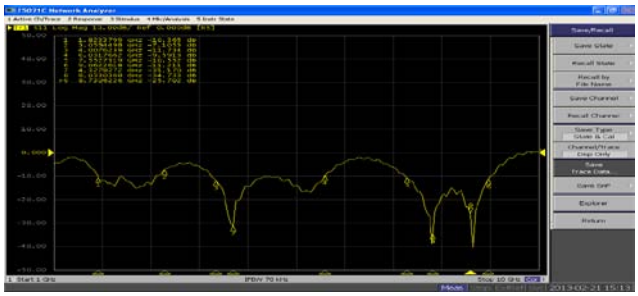

Figure-7. Return loss curve for wide octagonal strip monopole antenna using vector network Analyzer network.

VOL. 12, NO. 22, NOVEMBER 2017 ISSN 1819-6608
ARPN Journal of Engineering and Applied Sciences

www.arpnjournals.com

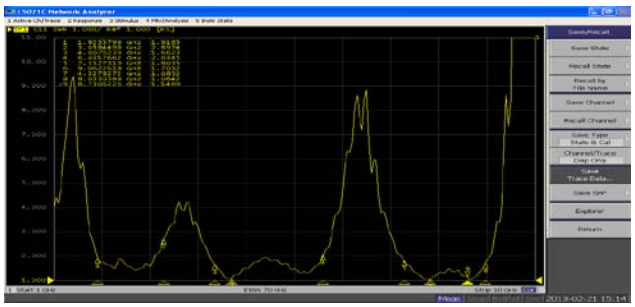

Figure-8. VSWR curve for wide octagonal strip monopole antenna using vector network analyzer network.

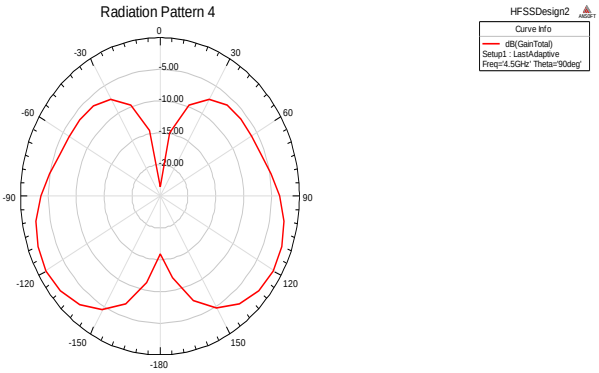

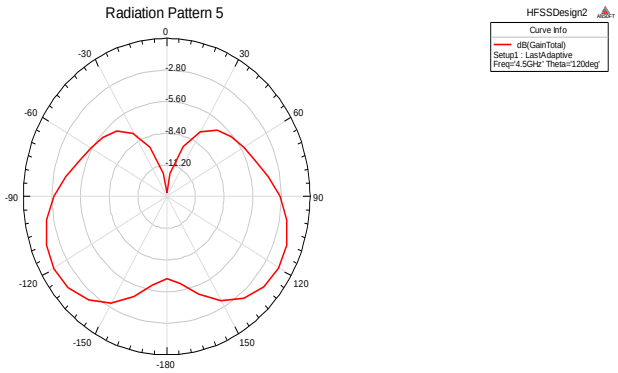

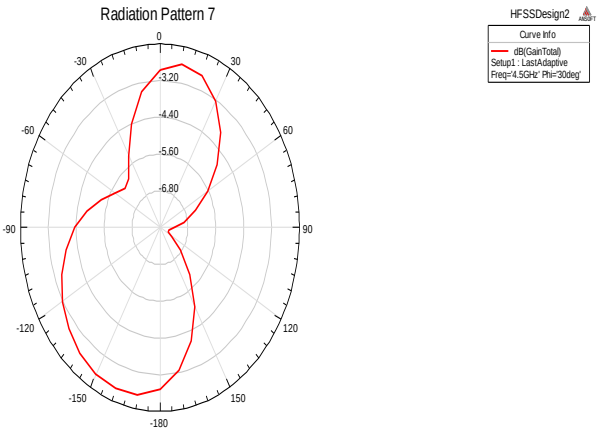

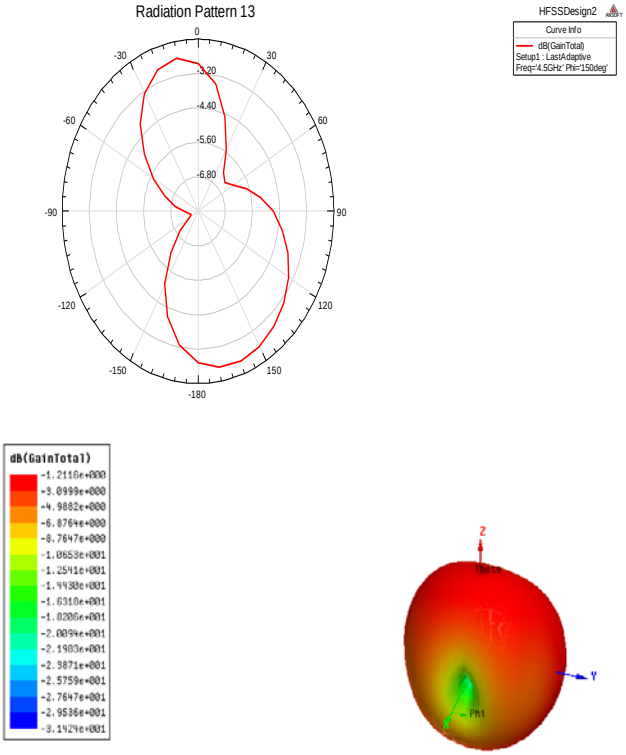

Figure-9. Mesured radiation patterns of hexagonal strip monopole antenna using HFSS at frequency of 1.94 GHz to 9.4 GHz

B. Hexagonal strip monopole antenna

The performance of the hexagonal shape antenna has been investigated by using HFSS. The figures 10, 11 shows the simulated return loss, VSWR and figures 12, 13 shows the tested return loss, VSWR and the figure-14 shows the radiation pattern of the strip monopole antenna from the frequency 1.34 GHz to 5.65 GHz.

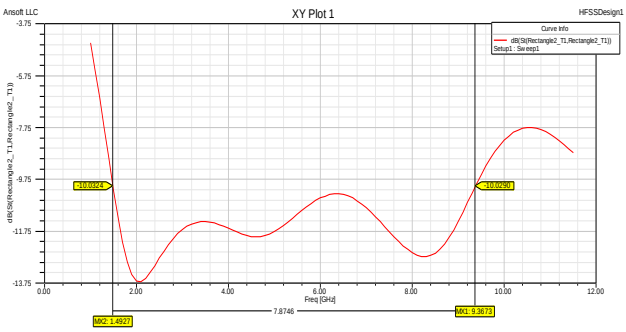

Figure-10. Return loss curve for wide hexagonal strip monopole antenna using HFSS.

VOL. 12, NO. 22, NOVEMBER 2017 ISSN 1819-6608
ARPN Journal of Engineering and Applied Sciences

www.arpnjournals.com

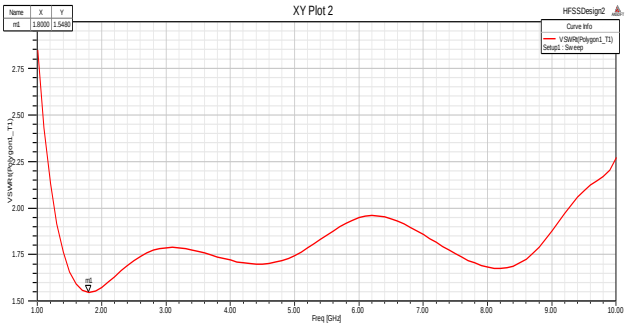

Figure-11. VSWR curve for wide octagonal strip monopole antenna using HFSS.

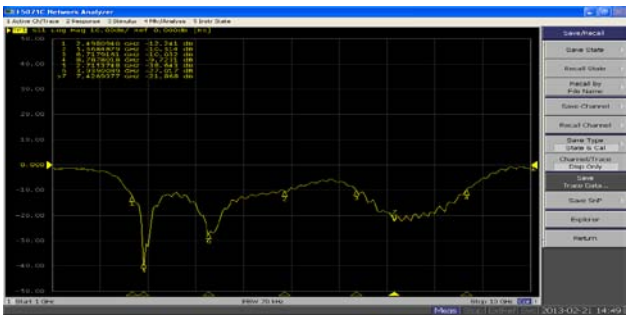

Figure-12. Return loss curve for wide hexagonal strip monopole antenna.

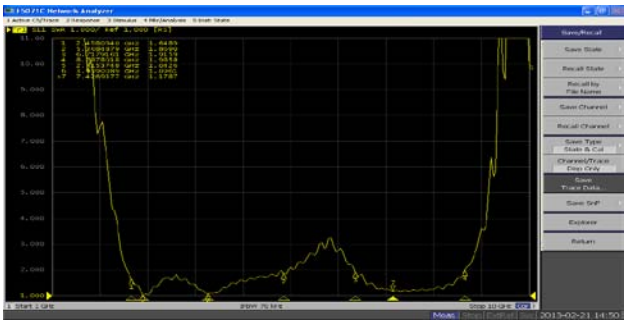

Figure-13. VSWR curve for wide hexagonal strip monopole antenna.

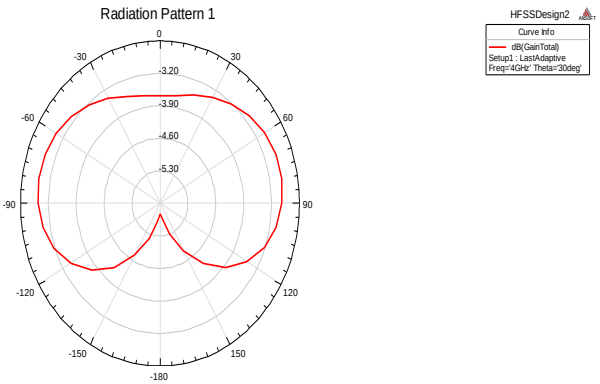

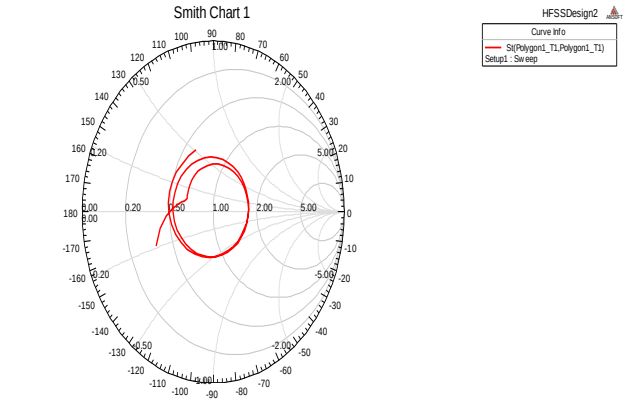

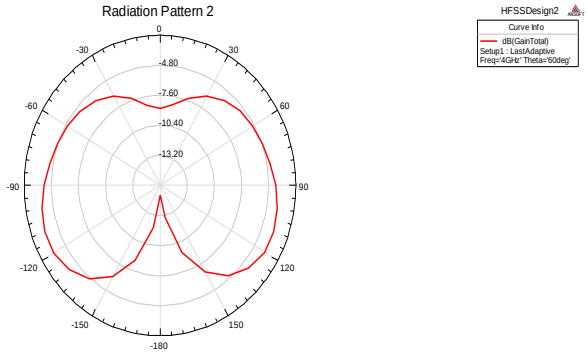

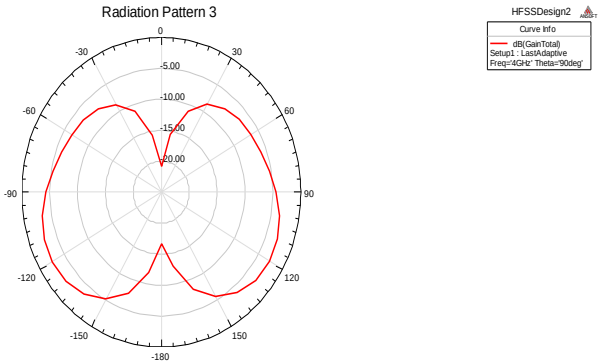

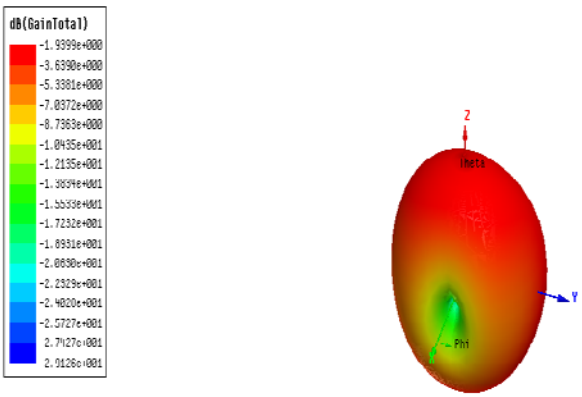

Figure-14. Measured radiation patterns of octagonal strip monopole antenna using HFSS at frequency of 1.3GHz to 5.65GHz.

5. CONCLUSIONS

The proposed work is mainly useful to operate the antenna at a particular band of frequencies. The hexagonal and octagonal shaped antennas has been built and simulated using the Ansoft HFSS and the practical results are obtained by testing the fabricated antennas on vector network analyzer (E5071C). The hexagonal strip monopole is resonating at 5.5 GHz and UWB impedance bandwidth ($S11 < -10$ dB) ranges from 1.54 to 9.41GHz, is observed in simulation result where as in practical results observed at 2.4 GHz to 8.7GHz. While the octagonal strip monopole is resonating at 5.5GHz and UWB impedance bandwidth ($S11 < -10$ dB) ranges from 1.3 to 5.65 GHz, is observed in simulation result whereas in practical results observed in steps of 3 bands 1.8GHz-3GHz, 4GHz-6GHz and 7GHz-9GHz. The VSWR values for hexagonal is 1.52:1 at 2.09GHz & for Octagonal it is 1.53:1 at 1.78GHz. The bandwidth for hexagonal is 7.87GHz, while for octagonal is 4.35GHz.The proposed antennas provides nearly omni-directional radiation characteristics with moderate gain and efficiency which is suitable for the next generation ultra wide-band applications.

REFERENCES

[1] 2002. FCC 1st Report and Order on Ultra-Wideband Technology.

[2] Schantz H. 2005. The Art and Science of Ultra wideband antennas, Artech House.

[3] A. Balanis. 2005. Antenna theory: analysis and design /Constantine, third edition, Hoboken, NJ: Wiley, ISBN 047166782X (hbk.).

[4] Ross Kyprianou, Bobby Yau and Aris. 2006. Investigation into Novel Multi-band Antenna Design. Defence science and Technology organization, Australia.

[5] C. I. Lin and K. L. Wong. 2007. Printed monopole slot antenna for internal multiband mobile phone antenna. IEEE Trans. Antennas Propag. 55(12): 3690-3697.

[6] A. Cabedo, J. Anguera, C. Picher, M. Ribo, and C. Puente. 2009. Multiband handset antenna combining a PIFA, slots, and ground plane modes. IEEE Trans. Antennas Propag. 57(9): 2526-2533.

[7] J. Anguera, I. Sanz, J. Mumbru, and C. Puente. 2010. Multiband handset antenna with a parallel excitation of PIFA and slot radiators. IEEE Trans. Antennas Propag. 58(2): 348-356.

[8] L. H. Weng, Y. C. Guo, X.W. Shi and X. Q. Chen. 2008. An overview on defected ground structure. Progress in electromagnetic Research B. 7: 173-189.

[9] 2007. Microstrip patch antenna. www. electronicshome.com.

[10] D. M. Pozar and D. H. Schaubert. 1995. Microstrip Antennas, the Analysis and Design of Microstrip Antennas and Arrays. IEEE Press, New York, USA.

[11] D. Krishna and M. Gopikrishna. 2009. Compact wideband koch fractal printed slot antenna. IET Microwave Antenna and Propagation. 3: 782-789.

[12] K. Yen and L. Hanzo. 2004. Genetic-algorithm-assisted multiuser detection in asynchronous CDMA communication. IEEE Transactions on Vehicular Technology. 53(5).

[13] M. Ding and R. Jin. 2007. Design of CPW-fed ultra wideband fractural antenna. Microwave and Optical Technology Letters. 49: 173-176.